Ninth International Conference on CFD in the Minerals and Process Industries
CSIRO, Melbourne, Australia
10-12 December 2012

SIMULATION STUDY ON THE HYDRODYNAMIC CHARACTERISTICS OF MEMBRANE-ASSISTED MICRO-FLUIDIZED BEDS

Lianghui Tan[1], Martin van Sint Annaland[1*]

[1]Multiphase Reactors Group, Department of Chemical Engineering and Chemistry,
Eindhoven University of technology , P.O. Box 513, 5600 MB Eindhoven, The Netherlands
*Corresponding author, E-mail address: m.v.sintannaland@tue.nl; Tel: (+31) 40 247 2241;Fax: (+31) 40 247 5833

ABSTRACT

Recent research has shown the great potential of membrane-assisted fluidized bed reactors for various applications, and for ultra-pure hydrogen production in particular. To maximize the installed membrane area per unit volume, the concept of micro-structured membrane-assisted fluidized bed reactor (MMAFBR) has been proposed. For a proper reactor design, numerical simulations with a discrete particle model have been carried out to investigate the effects of gas permeation in one membrane-assisted micro-fluidized bed (MAMFB) compartment.

It has been found that gas addition or extraction via walls confining the emulsion phase have a very pronounced influence on the bed hydrodynamics. With a fixed outlet superficial gas velocity, reversed solids circulation pattern in MAMFB with gas addition and densified zones close to the membrane walls in MAMFB with gas extraction have been observed. Moreover, gas permeation can cause gas bypassing, which deteriorates the fluidization properties and gas-solid contacting and hence the reactor performance.

NOMENCLATURE

d_p	Particle diameter	m
e_n, e_t	Normal and tangential coefficient of restitution	-
$\vec{F}_{c,a}$	Contact force of particle a	N
$\vec{g}$	Gravitational acceleration	m/s^2
I_a	Moment of inertia	kg·m
k_n	Normal spring stiffness	N/m
k_t	Tangential spring stiffness	N/m
T_a	Torque of particle a	N·m
m_a	Mass of particle a	kg
V_a	Particle volume	m^3
f_a	Volume fraction of particle a in a grid cell	-
M_g	Molar mass of gas	kg/mol
R	Gas constant	J/(mol·K)
Re_s	Reynolds number	-
$\vec{u}_g, \vec{v}_a$	Gas and solid velocity	m/s
p	Pressure	kg/(m·s^2)
T_g	Gas Temperature	K
V_{cell}	Volume of the cell	m^3
u_g	Superficial gas velocity	m/s
u_{mf}	Minimum fluidization velocity	m/s
β	Drag coefficient for a control volume	kg/(m^3·s)
ρ_g	Gas density	kg/m^3
ρ_p	Particle density	kg/m^3
μ_g	Fluid viscosity	Pa·s
ω_a	Angular velocity	rad/s
ε_g	Voidage	-
ε_s	Solid volume fraction	-
μ_f	Friction coefficient	-

INTRODUCTION

Membrane-assisted fluidized bed reactors have been one of the most attractive reactor types for various applications due to the excellent separation properties of membranes and good hydrodynamic properties of the fluidized bed (i.e. uniform temperature and excellent mass and heat transfer). In particular for hydrogen production, membrane-assisted fluidized bed reactors have been recognized as a very promising reactor concept in contrast to conventional fixed bed steam methane reforming reactors (Adris et al., 1991; Adris et al., 1994; Deshmukh et al., 2007a;). Previous studies have clearly demonstrated the theoretical and technical feasibility of producing ultra-pure hydrogen by integrating carbon dioxide capture into membrane-assisted fluidized bed reactors (Patil et al., 2005, 2006 and 2007; Gallucci et al., 2008). However, two limitations in the performance of MAFBRs have been identified: i) the hydrogen permeation rate through the perm-selective membranes and ii) the mass transfer rate from the bubble phase to the emulsion phase (Deshmukh et al., 2007b; Patil et al., 2006, 2007; Gallucci et al., 2010a, 2010b). The first limitation can be overcome by inserting more membranes into the reactor. In this way, the membrane area per unit reactor volume will be increased, resulting in the concept of

micro-structured membrane-assisted fluidized bed reactors (MMAFBR). It is also possible to overcome the second limitation through a proper reactor design and operation optimization once the hydrodynamic and mass transfer characteristics of the MMAFB are understood. Considering the small scale, MMAFB will be a promising reactor concept to design a new reactor generation for ultra-pure H_2 production for PEMFC applications at smaller scales (typically 1-50kW).

The importance of detailed understanding of the hydrodynamics to a proper design of a reactor has been widely recognized. However, most experimental studies on membrane-assisted fluidized bed reactors are application-oriented in order to provide a proof-of-concept and to develop phenomenological models to assess the economic potential of MAFBRs. De Jong et al. (2011) performed an experimental study on the hydrodynamics in a pseudo-2D fluidized bed with inbuilt membranes in the walls confining the fluidized bed, and revealed largely changed solid circulation patterns and bubble size distribution profiles in membrane-assisted fluidized beds. Recently, computational fluid dynamics (CFD) has been widely used to improve our fundamental understanding on the hydrodynamics of fluidized beds. In particular, the discrete particle model (DPM) has been validated and extensively used for detailed understanding of hydrodynamic characteristics of gas-solid fluidized beds (for example, Goldschmidt et al., 2004; Ye et al., 2004). Most of the studies reported in literature using DPM are devoted to very small fluidized beds in contrast to experimental setups and pilot systems, due to the limitation of computational resources. Even so, numerical investigations on detailed effects of gas permeation through membranes on the hydrodynamic characteristics of membrane-assisted micro-fluidized beds (MAMFBs) have hardly been reported. Considering the size of and the gas-solid system in MAMFBs, a state-of-the-art DPM model is currently the most suited model for this study, since it takes the fluid-particle drag and particle-particle interactions (both restitution and friction) into account in detail, while it still allows the hydrodynamic properties of a fluidized bed (such as larger scale solids circulation patterns and bed porosity profiles) to be investigated.

This study has been carried out in order to get detailed information on the hydrodynamic characteristics of one membrane-assisted micro-fluidized bed (MAMFB) compartment which is important for the design of such a reactor. Investigation on the influences of gas permeation through membranes, which are built into two walls confining the gas-solid suspension, on the hydrodynamic characteristics of MAMFBs has been carried out with the DPM model. Comparing to the fluidized bed without gas permeation, the greatly changed solids circulation patterns and solids holdup distribution have been found when gas is added or extracted via membrane walls. Moreover, the membrane area obviously plays a role in the investigation of the influences of gas permeation on the hydrodynamic characteristics of MAMFBs.

NUMERICAL MODELLING

Discrete particle model

The soft-sphere DPM employed in this study has originally been developed by Hoomans et al. (1996) and Ye et al. (2004). For the solid phase, each particle is tracked individually using Newton's second law of motion and for the gas phase, the volume-averaged Navier-Stokes equations are solved to calculate gas-phase hydrodynamics. The interphase coupling representing fluid-particle interactions is done with the fluid drag correlation. The in-house developed code was used to study the hydrodynamic characteristics of fluidized bed with Geldart A particles (Ye et al., 2004, 2005; Wang et al., 2010) which are also used in this work. The main equations of this model are summarized in table 1, where the contact forces resulting from particle-particle and/or particle-wall interactions are calculated using the linear spring and dashpot model proposed by Cundall and Strack (1979) and the gas-particle drag is computed with the correlation derived from extensive lattice Boltzmann simulations (Beetstra et al., 2007). According to Wang et al. (2010), in the soft-sphere DPM, variations of these parameters of particle-particle interactions do not bring any significant change in the predicted fluidization behavior in bubbling gas-fluidized beds of Geldart A type particles. To reduce the required CPU time (usually in the order of 10^{-5}s), the parameters of particle-particle interaction are usually set to values which are much smaller than the ones derived from material properties (Tsuji et al., 1993). Here, we choose those values to ensure that the maximal overlap between interacting particles (including the walls) at any time step is less than one percent of the particle diameter. Those values have been verified and used in previous studies in predicting the fluidization behavior in gas-fluidized beds of Geldart A type particles (Wang et al. 2010, 2011). The size of the Eulerian grid cells for the gas phase is larger than particle size (grid size of 0.2mm×0.2mm×0.2mm). Note that with the selected grid size the grid spacing was found to have a negligible influence on the derived fluidization characteristics. The algorithm to solve the hydraulic equations is a standard pressure correction technique.

Table 1: Main governing equations of the discrete particle model

Gas phase continuity equation:

$$\frac{\partial}{\partial t}\left(\varepsilon_g \rho_g\right) + \nabla \cdot \left(\varepsilon_g \rho_g \vec{u}_g\right) = 0$$

Gas phase momentum equations:

$$\frac{\partial}{\partial t}\left(\varepsilon_g \rho_g \vec{u}_g\right) + \nabla \cdot \left(\varepsilon_g \rho_g \vec{u}_g \vec{u}_g\right) = -\varepsilon_g \nabla p - \vec{S}_p + \nabla \cdot \left(\varepsilon_g \bar{\bar{\tau}}_g\right) + \varepsilon_g \rho_g \vec{g}$$

Gas phase equation of state:

$$\rho_g = \frac{M_g}{RT_g} p$$

Gas phase stress-strain tensor:

$$\overline{\overline{\tau}}_g = \mu_g\left(\nabla\vec{u}_g + \nabla\vec{u}_g{}^T\right) - \frac{2}{3}\mu_g\left(\nabla\cdot\vec{u}_g\right)\overline{\overline{I}}$$

Gas-solid momentum exchange rate:

$$\vec{S}_p = \frac{1}{V_{cell}}\sum_{\forall a\in cell}\frac{\beta V_a}{1-\varepsilon_g}\left(\vec{u}_g - \vec{v}_a\right)\delta\left(r - r_a\right)$$

$$\beta = 180\frac{\mu_g\varepsilon_s^2}{d_p^2\varepsilon_g} + 18\frac{\mu_g\varepsilon_g^3\varepsilon_s\left(1+1.5\sqrt{\varepsilon_s}\right)}{d_p^2}$$

where

$$+0.31\frac{\mu_g\varepsilon_s\,\mathrm{Re}_s}{\varepsilon_g d_p^2}\frac{\left[\varepsilon_g^{-1} + 3\varepsilon_g\varepsilon_s + 8.4\,\mathrm{Re}_s^{-0.343}\right]}{\left[1+10^{3\varepsilon_s}\,\mathrm{Re}_s^{-0.5-2\varepsilon_s}\right]}$$

$$\text{and } \mathrm{Re}_s = \frac{\varepsilon_g\rho_g d_p\left|\vec{u}_g - \vec{v}_a\right|}{\mu_g}$$

the porosity in DPM simulation:

$$\varepsilon_g = 1 - \frac{1}{V_{cell}}\sum_{\forall a\in cell} f_a V_a$$

Equations of motion for every particle:

$$m_a\frac{d\vec{v}_a}{dt} = -V_a\nabla p + \frac{V_p\beta}{1-\varepsilon_g}\left(\vec{u}_g - \vec{v}_a\right) + m_a\vec{g} + \vec{F}_{c,a}$$

$$I_a\frac{d\omega_a}{dt} = \mathrm{T}_a$$

Simulation layout

A fluidized bed of 3mm in width and 1.4mm in depth has been selected with two opposing vertical walls acting as membranes for gas addition and extraction. The height of the membranes and the simulated domain are 5mm and 18mm respectively. This fluidized bed resembles a compartment of a membrane micro-structured fluidized bed reactor. Monodisperse Geldart A type particles with diameter of 75μm (1500kg/m^3) were simulated using air as fluidizing agent with superficial gas velocity of 0.05 m/s. For the cases of the fluidized bed with gas permeation (i.e. 140%-40%$^{(a)}$, 120%-20%$^{(a)}$, 80%+20%$^{(a)}$ and 60%+40%$^{(a)}$ where the first number indicates the amount fed via the bottom distributor relative to the reference case without gas permeation and the second number indicates the relative amount extracted (-) or fed (+) via the membranes, and $^{(a)}$ indicates that the membranes were assumed in the left and right walls), the outlet superficial gas velocity at the top of the bed has been kept constant and equal to its reference case by adjusting the background velocity to the amount of gas permeated via the membranes. The reference case (100%±0%) is the same fluidized bed without gas permeation through the membranes. In order to investigate the influence of membrane area, calculations (cases indicated with $^{(b)}$) were performed where it was assumed that the membranes were built in the front and back walls which have a larger surface area compared to the left and right walls (1.5×10^{-5}m^2 vs 7.0×10^{-6}m^2) with the same height of 5mm as well. As shown in table 3, simulations (140%-40%$^{(b)}$, 120%-20%$^{(b)}$, 80%+20%$^{(b)}$ and 60%+40%$^{(b)}$) with the same outlet superficial gas velocity of 0.05m/s and gas permeation ratio use a lower permeation velocity because of the increased membrane surface area. All parameters used in this study have been summarized in Table 2 and all simulation series are summarized in Table 3.

Table 2: Summary of the parameters used in the discrete particle simulations

Particle diameter d_p, μm	75
Particle number Npart	42000
Particle density ρ_p, kg/m^3	1500
Restitution coefficients e_n, e_t	0.95
Friction coefficient μ_f	0.3
Normal spring stiffness k_n, N/m	7
Tangential spring stiffness k_t, N/m	2
CFD time step, s	1.0×10^{-5}
Particle dynamics time step, s	1.0×10^{-6}
domain height, m	1.8×10^{-2}
domain width, m	3.0×10^{-3}
domain depth, m	1.4×10^{-3}
Membrane length, m	5.0×10^{-3}
Superficial gas velocity u_g, m/s	0.05
minimum fluidization velocity u_{mf}, m/s	0.0035
Number of grid cells	90×15×7

Table 3: Summary of the simulation series

Simulation name	Background gas flow/velocity		Total membrane flow/velocity		Membrane position
	[%]	[m/s]	[%]	[m]	[-]
Reference	100	0.05	0	0	Left/right wall
80%+20%$^{(a)}$	80	0.04	+20	0.003	
60%+40%$^{(a)}$	60	0.03	+40	0.006	
120%-20%$^{(a)}$	120	0.06	-20	-0.003	
140%-40%$^{(a)}$	140	0.07	-40	-0.006	
Reference	100	0.05	0	0	Front/back wall
80%+20%$^{(b)}$	80	0.04	+20	0.0014	
60%+40%$^{(b)}$	60	0.03	+40	0.0028	
120%-20%$^{(b)}$	120	0.06	-20	-0.0014	
140%-40%$^{(b)}$	140	0.07	-40	-0.0028	

Boundary and initial conditions have to be specified for the numerical simulations. At the top outlet, the pressure was specified at atmospheric pressure (101325 Pa). At the bottom inlet, a uniform prescribed gas velocity was imposed. At the membrane walls a prescribed normal velocity was imposed in case of gas permeation. At all walls without gas permeation the no-slip condition was imposed for the gas phase. Initially, particles were regularly packed at the bottom of the bed with zero average translational and rotational velocity plus a random fluctuating translational and rotational velocity. The tangential restitution coefficient was always set equal to the normal restitution coefficient and parameters for the particle-wall interaction were equal to the parameters for the particle-particle interaction, similar to our previous

simulation study on the regime transition in micro-fluidized beds (Wang et al., 2011).

INFLUENCE OF GAS PERMEATION

In this section, the simulation results will be analyzed based on the time-averaged results (from 2s to 7s simulation time). Subsequently, the effects of gas permeation on the hydrodynamic characteristics of MAMFBs, especially on the solids circulation patterns and solids holdup distribution, are presented and discussed.

Solids circulation patterns

In this study, the computed time-averaged solids circulation patterns are shown in 3D graphs consisting of cross-sectional contours of the axial solid phase velocity at different bed heights and a contour plot of the solids velocity in the center computational cells in the depth direction. Fig.1 shows the solids circulation patterns for MAMFBs, where the outlet superficial gas velocity was kept constant at 0.05m/s and operated in the bubbling fluidization regime, where gas extraction or gas addition was imposed at the left and right walls: 140%-40%[(a)], 120%-20%[(a)], the reference, 80%+20%[(a)] and 60%+40%[(a)] cases. In this figure, the well-known solids circulation pattern that solids flow upwards through the center and fall down along walls can be clearly discerned for the reference case. However, clearly distinct solids circulation patterns were found for fluidized beds with gas addition and extraction: in case of gas extraction via the walls the upflow region becomes much more concentrated in the centre, while with gas addition the solids circulation is even inverted, i.e. downflow in the centre and upflow of solids along the walls. Those qualitative findings correspond well to the experimental results by De Jong et al (2011).

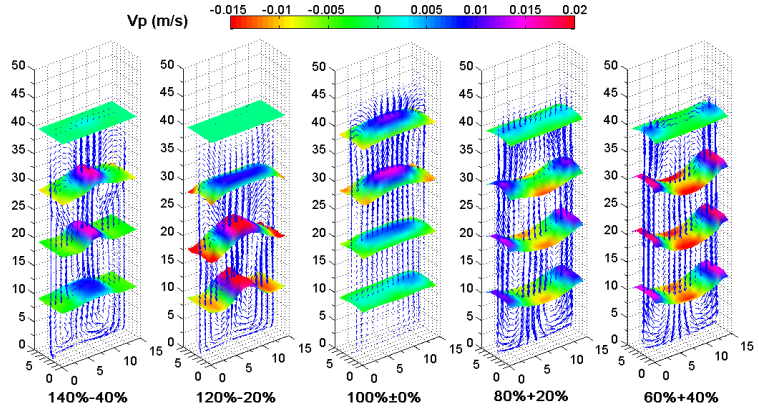

Figure 1: Solid circulation patterns in fluidized beds with an outlet superficial gas velocity of 0.05m/s and gas permeation imposed through the left and right walls

The results from the cases where gas extraction or gas addition was imposed at the front and back walls: 140%-40%[(b)], 120%-20%[(b)], the reference, 80%+20%[(b)] and 60%+40%[(b)] show very similar, but much less pronounced effects of gas permeation, due to the decreased gas permeation velocities. In Fig.2, a similar solids circulation pattern for the case with gas extraction and more complicated solids circulation pattern for the case with gas addition can be discerned. A careful observation shows the reversed solids circulation pattern in the panel parallel to the direction of gas addition.

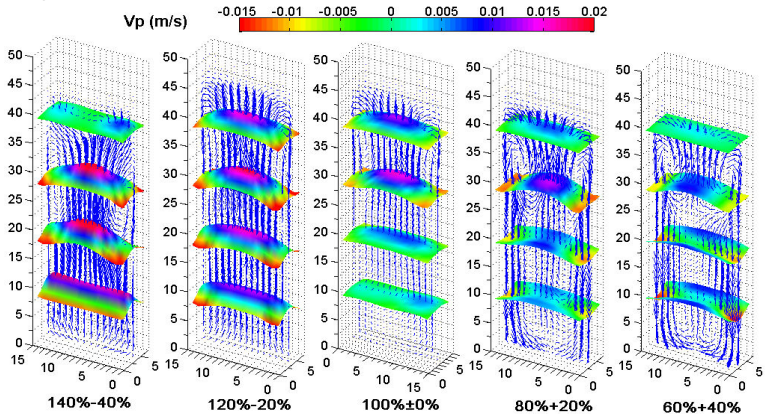

Figure 2: Solid circulation patterns in fluidized beds with an outlet gas velocity of 0.05m/s and gas permeation imposed through the front and back walls

Solids holdup distribution

Fig.3 shows the solids holdup distribution which is averaged over the bed in the direction of no gas permeation for the cases with gas permeation imposed on the left and right walls. Quite different from the reference case, it seems that stagnant (very) densified zones, where the solids holdup reaches values up to the value of a random packed bed with monodisperse particles, appear close to membrane walls in the fluidized bed with gas extraction. Similar phenomena have been found by De Jong et al. (2011) in their pseudo-2D experimental studies on much larger membrane-assisted fluidized beds. Actually, the particles in the densified zones close to membrane walls in Fig.3 are moving, which can be validated in Fig.4 which shows snapshots of the fluidized beds at different moments in time with zooming in the densified zone close to the left wall and the particles are colored in order to discern the change of position. In case of gas addition, the solids holdup increases relatively uniformly throughout the bed center, but decreases close to membrane walls (see Fig.3).

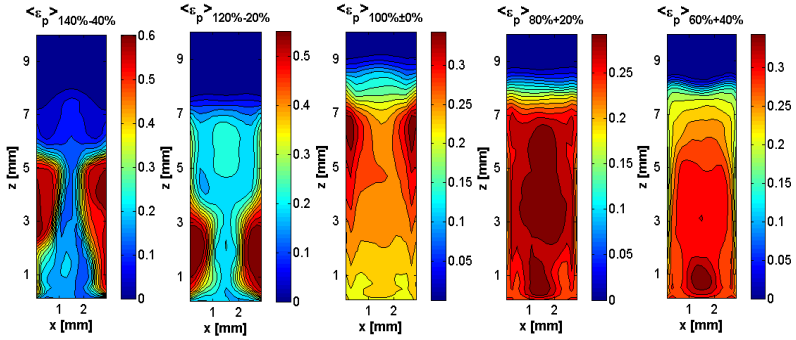

Figure 3: Time-averaged solids fraction in fluidized beds with outlet gas velocity of 0.05 m/s and gas permeation imposed through the left and right walls

For the cases with gas permeation imposed on the front and back walls, similar but much less pronounced phenomena can also be observed in Fig.5 for solids holdup distribution, i.e. relative densified zones for the cases with gas extraction and relative low solids holdup for the cases with gas addition close to the membrane walls, especially for the cases with a high gas permeation ratio. The very densified zones, where the values of solids holdup close to the value of a random packed bed with monodisperse particles, appear close to membrane walls can only be discerned for the case of 140%-40%[(b)].

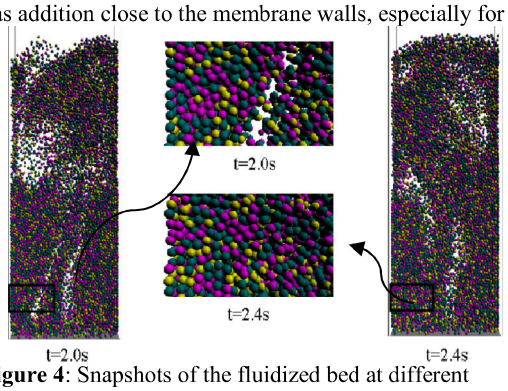

Figure 4: Snapshots of the fluidized bed at different moments in time with gas extraction through the left and right walls for the case of 20% gas extraction

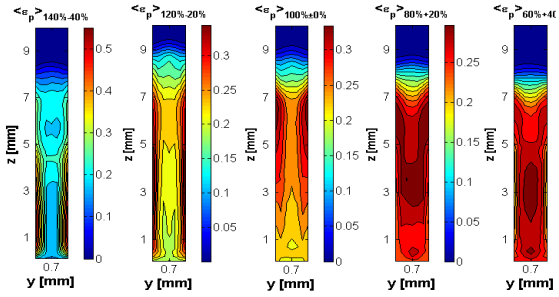

Figure 5: Time-averaged solids fraction in fluidized beds with outlet gas velocity of 0.05 m/s and gas permeation imposed through front and back walls

DISCUSSION AND CONCLUSIONS

The influences of gas permeation through membranes in the opposing vertical walls confining the fluidized bed on the hydrodynamic characteristics of MAMFBs have been investigated in the bubbling fluidization regime with the DPM model. The influences of both gas addition and extraction on the solids circulation patterns and solids holdup distribution have been computed and analyzed with different membrane areas but the same bed geometry.

Comparing to reported experimental results, similar effects of gas permeation on the hydrodynamic characteristics of MAMFBs in the bubbling fluidization regime have been revealed. Qualitatively consistent densified zones close to the membranes in MAMFBs with gas extraction and reversed solids circulation patterns in MAMFBs with gas addition have also been found in this numerical study. Gas extraction imposed to MAMFBs causes the solids holdup close to the membrane walls increase and much densified zones may be created with increasing gas extraction velocity. It is necessary to point out that particles in the densified zones close to membrane walls are moving with certain velocities. On the other hand, gas addition imposed to MAMFBs has a contrary effect on the solids behavior comparing to the reference case without gas permeation. A

reversed solids circulation pattern can be easily achieved when the amount of gas added is high enough. Opposite to the higher solids holdup close to the membrane walls caused by gas extraction, a higher solids holdup is found in the bed center for the cases with gas addition. Similar phenomena have been observed for the cases where membranes were assumed built in the front and back walls with high membrane area. A primary conclusion that the influence of gas permeation decrease with decreasing permeation ratio or increasing membrane area is obtain.

Based on the contours of solids holdup distribution both for gas extraction and gas addition, gas bypassing can be predicted since the dilute regions in the bed centre for the cases with gas extraction and close to membrane walls for the cases with gas addition are the easy paths for the gas to flow through with high velocity. Therefore, gas bypassing and a reduced residence time of the gas phase can be triggered by gas permeation via the membranes in MAMFBs for both gas addition and extraction, which is detrimental for the fluidization properties and gas-solid contacting and hence the reactor performance.

This numerical study is a starting point for the research on the design of a real MMAFBR and these primary results illuminate the unique hydrodynamic characteristics of one membrane-assisted micro-fluidized bed (MAMFB) compartment. The formation of densified zones close to membrane for the case of gas extraction may create an additional resistance for the mass transfer and gas-bypassing caused by gas addition via membrane will deteriorate the reactor performance. Therefore, the reactor design requests a careful tuning of the membrane area, permeability and superficial gas velocity, which should be based on detailed understanding of the hydrodynamics. Therefore, it is necessary to carry out further studies on the hydrodynamic characteristics of MAMFBs under different operation conditions, and to investigate the influence of hydrodynamics on the heat and mass transfer inside the bed and between the bed and the membranes.

REFERENCES

ADRIS, A.M., ELNASHAIE, S.S.E.H., HUGHES, R., (1991), "A fluidized bed membrane reactor for the steam reforming of methane", Can.J.Chem.Eng., 69, 1061-1070.

ADRIS, A.M., LIM, C.J., GRACE, J.R., (1994), "The fluidized bed membrane reactor system: a pilot scale experimental study", Chemical Engineering Science, 49 (24), 5833-5843.

BEETSTRA, R., VAN DER HOEF, M.A., KUIPERS, J.A.M., (2007), "Drag force of intermediate Reynolds number flow past mono- and bidisperse arrays of spheres", AIChE J., 53, 489-501.

CUNDALL, P.A. and STRACK, O.D.L., (1979), "A discrete numerical model for granular assemblies", Géotechniques, 29, 47-65.

DE JONG, J.F., VAN SINT ANNALAND, M., and KUIPERS, J.A.M., (2011), "Experimental study on the effects of gas permeation through flat membranes on the hydrodynamics in membrane-assisted fluidized beds", Chemical Engineering Science, 66, 2398-2408.

DESHMUKH, S.A.R.K, HEINRICH, S., MÖRL, L., VAN SINT ANNALAND M., KUIPERS J.A.M., (2007a), "Membrane assisted fluidized bed reactors: Potentials and hurdles", Chemical Engineering Science, 62, 416-436.

DESHMUKH, S.A.R.K., VAN SINT ANNALAND, M., and KUIPERS, J.A.M., (2007b), "Gas back-mixing studies in membrane assisted bubbling fluidized beds", Chemical Engineering Science, 62, 4095-4111.

GALLUCCI, F., VAN SINT ANNALAND, M., and KUIPERS, J.A.M., (2008), "Autothermal Reforming of Methane with Integrated CO2 Capture in a Novel Fluidized Bed Membrane Reactor. Part 1: Experimental Demonstration", Topics in Catalysis, 51, 133-145.

GALLUCCI, F., VAN SINT ANNALAND, M., and KUIPERS, J.A.M., (2010a), "Theoretical comparison of packed bed and fluidized bed membrane reactors for methane reforming", International Journal of Hydrogen Energy, 35, 7142-7150.

GALLUCCI, F., VAN SINT ANNALAND, M., and KUIPERS, J.A.M., (2010b), "Pure hydrogen production via autothermal reforming of ethanol in a fluidized bed membrane reactor: A simulation study", International Journal of Hydrogen Energy, 35, 1659-1668.

GOLDSCHMIDT, M.J.V., BEETSTRA, R., and KUIPERS, J.A.M., (2004), "Hydrodynamic modeling of dense gas-fluidized beds: comparison and validation of 3D discrete particle and continuum models", Powder Technology, 142, 23-47.

HOOMANS, B.P.B., KUIPERS, J.A.M., BRIELS, W.J., VAN SWAAIJ, W.P.M., (1996), "Discrete particle simulation of bubble and slug formation in a two-dimensional gas-fluidized bed: a hard-sphere approach", Chemical Engineering Science, 51, 99-118.

PATIL, C.S., VAN SINT ANNALAND, M., KUIPERS, J.A.M., (2005), "Design of a Novel Autothermal Membrane-Assisted Fluidized-Bed Reactor for the Production of Ultrapure Hydrogen from Methane", Industrial & Engineering Chemistry Research, 44, 9502-9512.

PATIL, C.S., VAN SINT ANNALAND, M., KUIPERS, J.A.M., (2006), "Experimental Study of a Membrane Assisted Fluidized Bed Reactor For H2 Production by Steam Reforming of CH4", Chemical Engineering Research and Design, 84, 399-404.

PATIL, C.S., VAN SINT ANNALAND, M., KUIPERS, J.A.M., (2007), "Fluidised bed membrane reactor for ultrapure hydrogen production via methane steam reforming: Experimental demonstration and model validation", Chemical Engineering Science, 62, 2989-3007.

TSUJI, Y., KAWAGUCHI, T., and TANAKA, T., (1993), "Discrete particle simulation of two-dimensional fluidized bed", Powder Technology, 77, 79-87.

WANG, J., VAN DER HOEF, M.A., and KUIPERS, J.A.M., (2010), "The role of particle-particle interaction in bubbling gas-fluidized beds of Geldart A particles: a discrete particle study", Proceeding of AIP Conference, 1207 ed., 766-774.

WANG, J., Tan, L., van der Hoef, M.A., VAN SINT ANNALAND, M., and KUIPERS, J.A.M., (2011), "From bubbling to turbulent fluidization: Advanced onset of

regime transition in micro-fluidized beds", Chemical Engineering Science, 66, 2001-2007.

YE, M., VAN DER HOEF, M.A., and KUIPERS, J.A.M., (2004), "A numerical study of fluidization behavior of Geldart A particles using a discrete particle model", Powder Technology, 139, 129-139.

YE, M., VAN DER HOEF, M.A., and KUIPERS, J.A.M., (2005), "The effects of particle and gas properties on the fluidization of Geldart A particles", Chemical Engineering Science, 60, 4567-4580.